JOURNAL OF AIRCRAFT
Vol. 46, No. 4, July–August 2009

Unsteady Aerodynamic Coefficients Obtained by a Compressible Vortex Lattice Method

Fabiano Hernandes* and Paulo A. O. Soviero†
Instituto Tecnológico de Aeronáutica, 12228-900 São José dos Campos, Brazil

DOI: 10.2514/1.40610

Unsteady solutions for the aerodynamic coefficients of a thin airfoil in compressible sub- or supersonic flows were studied. The lift, the pitch moment, and the pressure coefficients were obtained numerically for the following motions: the indicial response (unit step function) of the profile, that is, a sudden change in the angle of attack; a thin profile penetrating into a sharp edge gust (for several gust velocity ratios); a thin profile penetrating into a one-minus-cosine gust, that is, a typical gust used in commercial aircraft design; the oscillating airfoil; and the interaction of the profile with a convected (from convection phenomenon) vortex passing under the profile, a phenomenon known in the literature as blade vortex interaction or, for a profile case, airfoil–vortex interaction. The present work uses a numerical approach based on vortex singularity. The numerical model was created through the profile discretization in uniform segments, and the compressible flow vortex singularity was used. The results available in the literature are based on approximated exponential equations or computed via computational fluid dynamics. Thus, the purpose of this method is to obtain results as accurate as those from approximated equations and significantly faster than those done via computational fluid dynamics.

Nomenclature

a	=	sound speed, m/s
c_p	=	dimensionless pressure coefficient
M	=	dimensionless Mach number
t	=	time, s
U	=	uniform velocity, m/s
w	=	induced velocity, m/s
α	=	angle of attack, rad
Γ	=	vorticity, m^2/s
Δc_p	=	dimensionless pressure coefficient jump
ϕ	=	velocity potential, m^2/s
$\delta\phi$	=	velocity potential jump, m^2/s

Subscripts

0	=	initial instant

I. Introduction

IT IS well known that linearized compressible aerodynamics and linearized acoustic equations can be derived from each other. Therefore, if a Galilean transformation is performed between two reference systems, one fixed to the airfoil and the other fixed to the still air at infinity, the elementary classical wave equation solutions, from acoustics, and the solutions of the convected wave equation can be obtained from the same transformation.

Extensive studies on elementary solutions for both wave and convected wave equations may be found in the literature [1–3]. In the past decade, the generalized vortex lattice method was developed for the unsteady motion for subsonic flows [4], initially, and later for supersonic [5] and transonic flows [6]. In all previous works, the profile motion (heaving or pitching) was restricted to the harmonic motion; thus, the calculation was done on the frequency domain.

If aerodynamic forces and moments on a thin profile are to be obtained for a given unsteady motion, there are three possible ways to solve the problem [7]. According to Bisplinghoff et al. [2], the first one is to use a superposition method (Fourier's integral) of the results obtained for harmonic motions. However, such a methodology is not adequate for sudden movements, which can happen during maneuvers of high-performance airplanes, sharp gusts, or fast deflections of command surfaces, such as the ailerons. In these cases, the number of terms in the series needed to describe forces and moment coefficients can become prohibitively large due to the slow convergence behavior of the solution describing the studied motion. The second approach is to superimpose indicial aerodynamic responses by means of the superposition principle embodied in Duhamel's integral [2]. In this case, the specified boundary conditions are satisfied in both the space and time domains. The third way consists of searching for the solution to the wave equation [7–9] or to the convected wave equation that fits the boundary conditions prescribed for the given motion [10]. It is this last procedure that will be used in this work.

The method used here was developed by Soviero and Hernandes [11] and considers the classical equation of the nonstationary aerodynamics (the convected wave equation). This method is the first methodology to use a simple numerical scheme to obtain forces and loads for an arbitrary motion of a profile in the unsteady compressible domain; to validate the method, a step change of the angle of attack (an indicial motion) was calculated. Here, the authors used the same method adapted to the boundary conditions used, including other relevant unsteady motions.

The method used is a simple and efficient numerical method based on point vortices. The main limitation of the procedure used is that the mathematical modeling corresponds to the two-dimensional potential linearized equations. The basis of the numerical procedure relies on the direct relationship between vortices and normal dipole panels with constant strength distribution.

In this work, the lift and pressure coefficients are obtained numerically for the following motions: 1) the indicial response (unit step function) of the profile, that is, a sudden change in the angle of attack; 2) a thin profile penetrating into a sharp edge gust (for several gust velocity ratios); 3) a thin profile penetrating into a one-minus-cosine gust, that is, a typical gust used in commercial aircraft design; 4) the oscillating airfoil; and 5) the interaction of the profile with a convected (from convection phenomenon) vortex passing under the profile, a phenomenon known in the literature as blade vortex interaction (BVI) or, for a profile case, airfoil–vortex interaction (AVI); such predictions are relevant mainly for helicopter projects,

Presented as Paper 4374 at the 38th Fluid Dynamics Conference and Exhibit, Seattle, Washington, 23–26 June 2008; received 27 August 2008; revision received 15 January 2009; accepted for publication 16 January 2009.

*Graduate Student, Aeronautical Engineering Division.
†Professor, Aeronautical Engineering Division. Senior Member AIAA.

for which the calculation of these loads is very important to determine the aeroelastic response and rotor aeroacoustics.

II. Compressible Vortex Lattice Method

The basic partial differential equation satisfied by the velocity potential in a three-dimensional fluid flow is derived from the Eulerian momentum equations, the continuity condition, and the relation for the speed of pressure propagation. These relations are all given analytically in Sears [12]. In a reference frame that translates steadily with uniform velocity, the perturbation velocity potential due to an arbitrary small-amplitude motion of a thin airfoil and wake is governed by the following linear convected wave equation:

$$\varphi_{xx}(1-M^2)+\varphi_{yy}+\varphi_{'zz}-2M/a\varphi_{xt}-1/a^2\varphi_{tt}=0 \qquad (1)$$

where the Mach number, M, is defined as the ratio of U and a.

The expression for the static pressure at any point in the flowfield is conveniently related to the freestream static and dynamic pressures as to form a dimensionless coefficient, c_p. Setting $c_p=(p-p_\infty)/(1/2\rho U^2)$ and imposing conditions consistent with the hypothesis of the small perturbation theory, it can be shown from Euler's equations that, provided the perturbation velocity components are of the same order of magnitude, the relation for the pressure coefficient is

$$c_p=-(2/U^2)(\varphi_t+U\varphi_x) \qquad (2)$$

Mirels and Haefeli [13] presented a method for calculating the velocity induced by vortex segments of any configuration for steady flow. Initially, an equation for compressible steady vortices in three-dimensional flow was performed. Then, a transformation based on the analogy between two-dimensional unsteady flow with three-dimensional steady flow [12] was done. Finally, another transformation was performed for the reference system fixed to the body in a moving environment.

The result is the following equation for induced velocity of a vortex element in a compressive environment with velocity U and the system fixed to the body:

$$w=\frac{K}{2\pi}\left\{\frac{\sqrt{T_1^2-1/a^2(X_1^2-UT_1^2)}}{T_1[X_1-T_1(U+m)]}-\frac{\sqrt{T_2^2-1/a^2(X_2^2-UT_2^2)}}{T_2[X_2-T_2(U+m)]}\right\} \qquad (3)$$

where $X_i=x-x_i$, $Y_i=y-y_i$, $Z_i=z-z_i$, and $T_i=t-t_i$.

Equation (3) presents two solutions of Eq. (1). The first one ($m=-U$) corresponds to a point vortex of constant strength Γ, generated impulsively in a uniform flow that remains fixed at certain position, that is, a bound vortex. The second solution ($m=0$) is a free vortex that is convected by the flow with uniform velocity U.

Figure 1 shows the induced velocities by the vortices in a steady environment and the transformations for the unsteady compressible flow in a rest environment and the system fixed to the body.

The proposed model is based on two well-known concepts of aerodynamic theory: 1) impulsive generation of vortices in a perfect fluid, and 2) the relation between a pair of contrarotating vortices and the velocity potential jump that occurs over the line that joins them.

The profile is divided into a convenient number of panels, n. The control points, at which the velocity potential jump $\delta\phi$ is applied, are placed in the center of each panel and identified by the index j (which varies between 1 and n, $1\le j\le n$). The time instants are identified by the index k, where k is worth 1 for the initial instant, $t_0=0$, until the final time at which $k=N$ (i.e., $1\le k\le N$). The variable dt corresponds to the passing time between interactions.

From the initial movement of the profile, an impulsive movement is generated over each panel, creating a potential jump $\delta\phi$. In the following instant, these perturbation potentials n are substituted by pairs of contrarotating vortices.

This sequence of events can be understood by referring to Fig. 2. The time $t=0$ ($k=1$) corresponds to an initial condition, for which the piston theory [2] is applied for the boundary condition over the profile with normal velocity of intensity U_n and the posterior substitution of potential jumps $\delta\phi$ by pairs of contrarotating vortices. For a posterior time ($t=dt$, $k=2$), the trailing-edge vortex moves at velocity U (by model imposition) and new potential jumps are calculated, now considering not only the normal velocity U_n but also the induced velocities by the vortices generated at instant $t=0^+$. For the other instants (up to the limit $k=N$), to calculate the induced velocities in each panel, every emitted vortice up to the instant before the considered instant must be considered. A sum of the bounded vortices is performed on the left edge of each panel.

The sequence of events for supersonic flow is analogous to that for subsonic flow, differing only because there is no emission of vortices created impulsively by the trailing edge, as all vortices are connected to the profile. The contrarotative vortices originating from the velocity perturbation potential jumps for the supersonic flow are all connected to the profile because the Kutta condition does not need to be respected in this regime. For the subsonic flow, the trailing-edge vortex of the profile (of intensity $-\Gamma_1^k$ situated at the right extremity of the panel $j=1$) is, by model imposition, free to automatically create a wake and satisfy the Kelvin's theorem.

It is possible to visualize the same time domain considering the time as an axis. This scheme permits a clearer understanding of its similarity with the vortex lattice method. This scheme is showed in Fig. 3.

Initially, an explicit model was studied in which the perturbation potential jumps were calculated as a direct function of the normal velocity over the panel at a given instant. And a boundary condition was established over the panel, that is, exactly over the control point of each panel. This concept proved to be inadequate because the convergence method depended directly on the time step used. More precisely, when a control point of a given panel was influenced by the vortex generated (at the left extreme of the panel) by the same panel at the preceding instant, the result presented oscillations and divergences in some cases. This divergence originated from the oscillations present in the curve of the pressure coefficient jump over the profile. The same oscillatory characteristic was observed by Hernandes and Soviero [14] and Long and Watts [9].

Because of these limitations, it was decided not to use an explicit model. The model was chosen to establish the boundary condition halfway through the considered instant and the instant immediately following it. Once again, the choice was based on the analogy between the 2-D unsteady regime and the 3-D steady regime, in which the point where the boundary condition is applied in the centroid of the panel is usually defined.

Therefore, the model becomes implicit because the considered control point is influenced by its own panel for the considered instant and its solution implies the solution of a linear system. Taking a coefficient matrix $[A]$ and multiplying it by the potential jumps matrix $[\delta\phi]^k$ for the considered instant k, the result is the boundary condition matrix $[W]^k$ (normal velocity over the panels):

$$[A][\delta\phi]^k=[W]^k \qquad (4)$$

The matrix $[A]$ is associated with the influence of the vortices generated at a given instant k and its influence at that instant. The elements of the main diagonal and the part related to the impulsion of the panel must also be summed, given by $1/2adt$.

For the subsonic flow, the velocity matrix $[W]^k$ is a function of the normal velocity to the profile due to movement ($U\alpha$) summed to the velocities induced by the emitted vortices at the instants before the considered instant. For the method to work properly in the supersonic regime, it is essential to consider the main element of the method: the vortex singularity. In the subsonic regime, it is possible to calculate the velocity induced by the vortex in any point of the area affected by it. Therefore, it is necessary to define the contribution of singularity to the velocity field. This concept is explored by Miranda et al. [15]. The part related to the induced velocity due to singularity is deduced from the induced velocity in the steady regime. Equations (5) and (6) show the resulting systems for the sub- and supersonic regimes, respectively:

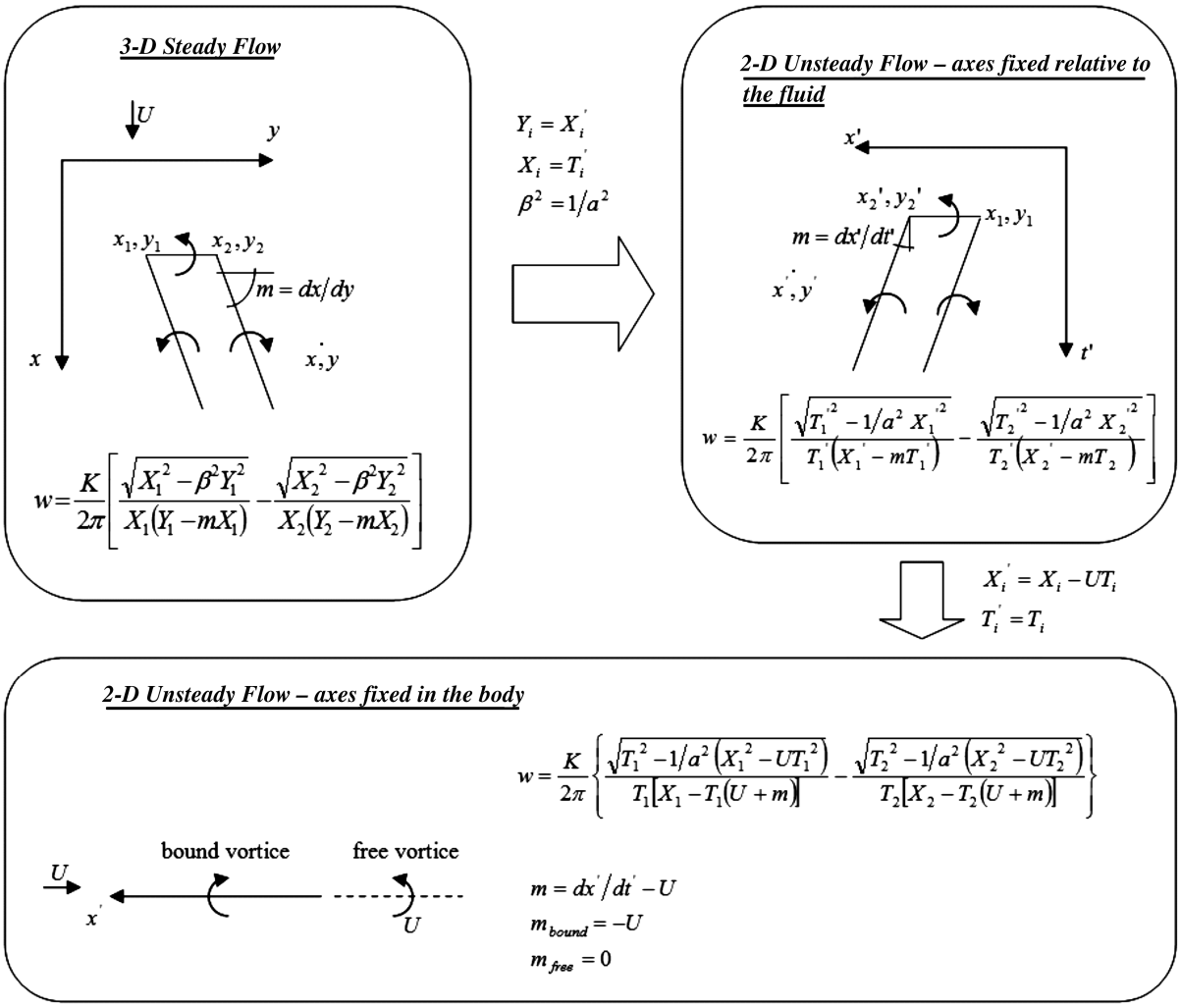

Fig. 1 System equivalence.

$$\begin{bmatrix} a_{11}+\frac{1}{2adt} & a_{12} & a_{1n} \\ a_{21} & a_{22}+\frac{1}{2adt} & a_{2n} \\ a_{n1} & a_{n2} & a_{nn}+\frac{1}{2adt} \end{bmatrix} \begin{bmatrix} \delta\phi_1^k \\ \delta\phi_2^k \\ \delta\phi_n^k \end{bmatrix} = \begin{bmatrix} U_n + \sum_{i=1}^{k-1}\sum_{j=1}^{n} w_1^{ji} \\ U_n + \sum_{i=1}^{k-1}\sum_{j=1}^{n} w_2^{ji} \\ U_n + \sum_{i=1}^{k-1}\sum_{j=1}^{n} w_n^{ji} \end{bmatrix} \tag{5}$$

$$\begin{bmatrix} a_{11}+\frac{1}{2adt} & a_{12} & a_{1n} \\ a_{21} & a_{22}+\frac{1}{2adt} & a_{2n} \\ a_{n1} & a_{n2} & a_{nn}+\frac{1}{2adt} \end{bmatrix} \begin{bmatrix} \delta\phi_1^k \\ \delta\phi_2^k \\ \delta\phi_n^k \end{bmatrix} = \begin{bmatrix} U_n + \sum_{i=1}^{k-1}\sum_{j=1}^{n} w_1^{ji} + \frac{\beta}{2}\sum_{i=1}^{k-1}(\delta\phi_1^i - \delta\phi_2^i) \\ U_n + \sum_{i=1}^{k-1}\sum_{j=1}^{n} w_{n-1}^{ji} + \frac{\beta}{2}\sum_{i=1}^{k-1}(\delta\phi_{n-1}^i - \delta\phi_n^i) \\ U_n + \sum_{i=1}^{k-1}\sum_{j=1}^{n} w_n^{ji} + \frac{\beta}{2}\sum_{i=1}^{k-1}\delta\phi_n^i \end{bmatrix} \tag{6}$$

From the solution of the system (matrix $[\delta\phi]^k$), the aerodynamic coefficient can be calculated.

III. Studied Motions

For incompressible flow, the indicial lift of a profile subjected to a sudden change in the angle of attack (step function) was obtained by Wagner [16]. The corresponding solution for the sharp edge gust in incompressible flow was obtained by Küssner [17]. Bisplinghoff et al. [2] present a synthesis of these results. In the study of aerodynamic loads in helicopter rotors, in situations in which the hypothesis of incompressibility can be applied, the Wagner and Küssner functions are used together with the Duhammel integral (Bisplinghoff et al. [2]), in which solutions for arbitrary motions in incompressible flow can be obtained through indicial functions (Wagner or Küssner). The study of gusts with variable propagation speed, for which intermediate solutions for the results of Wagner and Küssner were obtained, was developed by Miles [18] and Drischler and Diederich [19]; both studies make use of the Wagner function approaches to obtain their results. A numerical method to solve any incompressible flow motion was developed by Soviero and Lavagna [20].

The compressible flow may be divided into sub- and supersonic categories. For supersonic flow, the literature shows analytical solutions for the problems of a sudden change in angle of attack (Lomax et al. [21]) and a sharp edge gust (Heaslet and Lomax [22]). Bisplinghoff et al. [2] presented a summary of these results. In supersonic flow, studies of gusts with variable propagation velocity or of AVI (and BVI) were not observed. Although most of the studies concerning the application of gust and AVI (and BVI) were conducted with regard to the development of helicopter rotors, for which supersonic flow is not employed in the usual way, there is an application for these studies in the development of supersonic aircraft. Therefore, the supersonic flow considered in the present work is unknown in the literature.

The first studies in subsonic flow were developed by Lomax et al. [21], who obtained analytical solutions for pressure distribution, lift

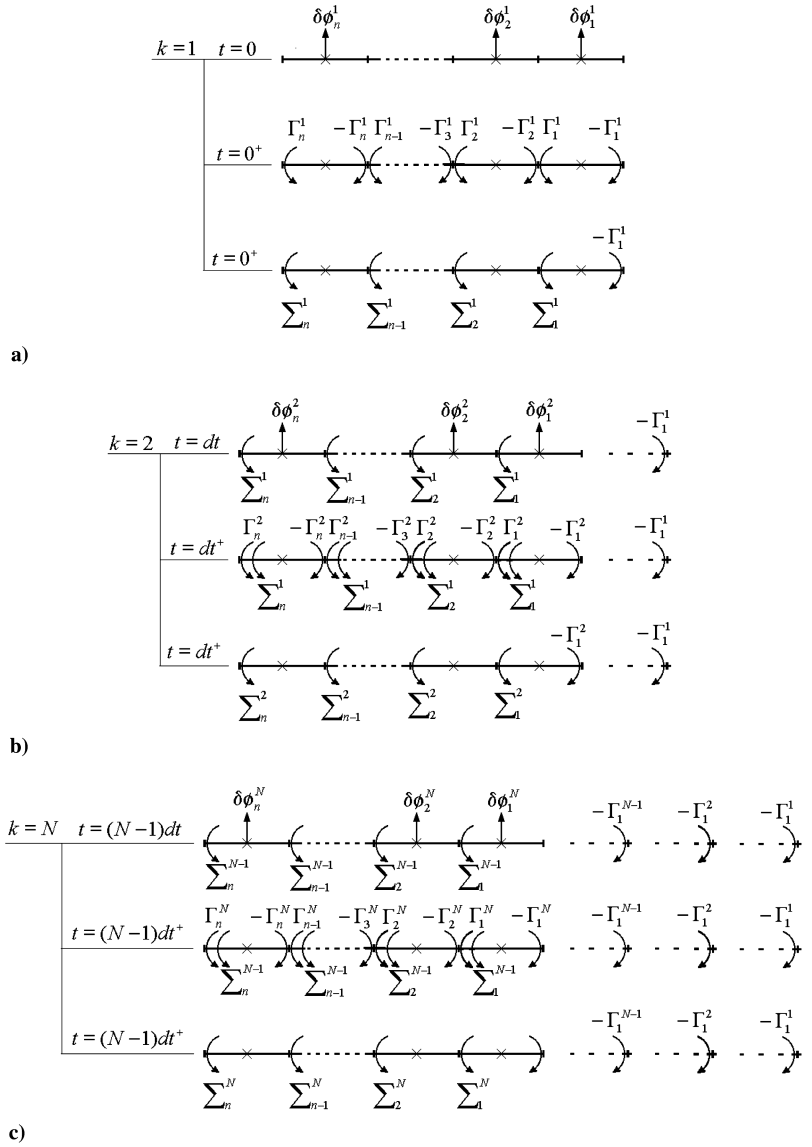

Fig. 2 Events sequence for subsonic flow: a) $k = 1$, b) $k = 2$, and c) $k = N$.

and pitch-up moments, and the step function; in an analogous way, Heaslet and Lomax [22] studied solutions for the sharp edge gust. However, the analytical results were only found for brief instants of time after the beginning of the motion, as the rest of this motion was completed by approximated functions, normally exponential functions. A numerical model for arbitrary compressible motions, based on the linearized acceleration potential, was developed by Long and Watts [9]. Numerical solutions of the Navier–Stokes equations were proposed by Shaw and Qin [23]. There are many studies that use an indicial function approach to obtain other motions, normally making use of superposition (see Beddoes [24] and Leishman [25]). Leishman [26], using reverse flow theorems, obtained results for gusts with variable propagation speed. Sitaraman and Baeder [27] obtained results for the AVI problem using computational fluid dynamics (CFD) and the superposition of indicial functions. The results of both studies were compared with our study. The gusts and AVI studies for profiles in subsonic flow have a direct application to the development of helicopters rotors.

Until the 1950s, the criteria for load calculation due to the presence of airplane gusts (or profiles) was based on the sharp edge gust model, that is, the aircraft suddenly suffers a vertical speed increase with definite intensity. With the development of airplanes with bigger dimensions and increased speed, the need to consider a dynamic-structural response was evident. A more proper discrete gust profile (that represents the existing atmospheric gusts) was defined for rigid body and dynamic structural analyses. The profile was defined as one-minus-cosine, and it is the profile studied here. Noback [28], Pratt and Walker [29], Flomenhoft [30], and Fuller [31] are good references concerning the historical evolution of gust profiles used in airplane projects.

The present study also studies the harmonic movement of lateral translation, that is, a rigid narrow profile submitted, without angle of attack variation, to a harmonic movement. Only the real part of the aerodynamic coefficients was calculated. Studies are being performed to complete the results with the imaginary part, because most methods of frequency domain and the results available in the literature calculate both parts: real and imaginary. The classical studies of Theodorsen [32] and Bisplinghoff et al. [2] are the available results provided in literature.

A. Step Function and Sharp Edge Gust

Let us consider a thin profile with zero angle of attack immersed in a uniform flow of velocity U. The profile is then submitted to a sharp edge gust of uniform intensity w_g (in the present work, the simplifying hypothesis of $w_g = U$, without loss of generality, was considered) moving relative to the uniform flow with velocity U_g. A gust velocity ratio, such as follows, was set:

$$\lambda = U/(U + U_g) \tag{7}$$

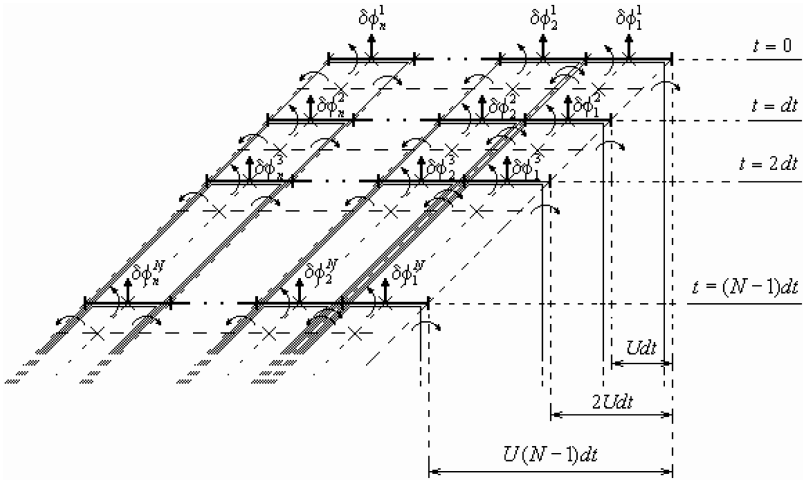

Fig. 3 Numerical scheme considering time as an axis, showing the vortex lattice appearance.

The velocity at which the gust comes into the profile is the sum of the velocities U and the relative gust velocity U_g; therefore, the gust moves over the profile with velocity $U + U_g = \lambda^{-1}U$. The boundary condition over the profile is then given by the normal velocity over it, which is the parts hit by the gust, $U_n = w_g = U$, and those still not hit by the gust $U_n = 0$. Figure 4 illustrates the gust problem.

Two typical cases of the gust velocity ratio, λ, will be discussed. When we have $\lambda = 0$ ($U_g \to \infty$), the solution of the problem results from the resolution of the step function problem (in which, at an instant $t = 0^+$, the whole profile is submitted to the gust and, similarly, to a sudden change in the angle of attack). And when $\lambda = 1$, which is called the classic sharp edge gust, the gust moves together with the flow over the profile. Both solutions are known in the literature as indicial responses and were already the object of previous study by the authors [33].

B. One-Minus-Cosine Gust (1 − cos)

Consider a thin profile with a zero incidence angle immersed in an environment with uniform velocity U. The profile is then submitted to a gust of intensity $U_{1-\cos}(s)$, according to the profile called one-minus-cosine. The profile one-minus-cosine discrete gust is defined as

$$U_{1-\cos}(s) = \begin{cases} \frac{\bar{U}_{1-\cos}}{2}[1 - \cos(\frac{2\pi s}{2H})], & 0 \le s \le 2H \\ 0, & s > 2H \end{cases} \tag{8}$$

where s denotes the dimensionless distance of gust penetration, $s = Ut/c$. The intensity of the gust is defined by $\bar{U}_{1-\cos}$ and, in the present work, by $U = \bar{U}_{1-\cos}$. In airplane projects, the prescribed values [25] for the gust intensity are 50 ft/s for altitudes between sea level and 20,000 ft, decreasing to 25 ft/s at 50,000 ft. H denotes the gust gradient, that is, the distance parallel to the axis of gust displacement where gust intensity is maximum. A significant number of H values must be used in projects to determine critical values that maximize the profile (or airplane) load. For the problems studied here, the following values were used: $2H = 5$ and 25. The results were compared with those of Zaide and Raveh [34], in which the results for a one-minus-cosine gust were obtained from a process of data convolution obtained by CFD for the sharp edge gust. Figure 5 illustrates the problem of the one-minus-cosine gust.

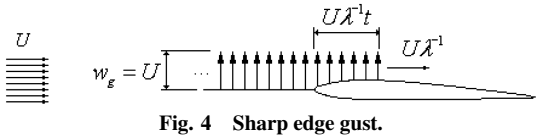

Fig. 4 Sharp edge gust.

C. Harmonic Movement

The present work studied the harmonic translation movement of a thin profile in an environment with uniform velocity U, which oscillates vertically with zero angle of attack according to function $h(t)$, defined as follows:

$$h(t) = h_0 \text{sen}(wt) \tag{9}$$

The oscillation frequency is defined by $w = 2k_r U/c$, where k_r is the reduced oscillation frequency. For the present work, the following was used: $h_0 = U/2$ and $k_r = \pi/5$ (this value was used as a reference only, because it implies a period equal to a minus-sine gust). Figure 6 illustrates the harmonic translation movement.

D. Airfoil–Vortex Interaction

The AVI problem consists of studying the interaction of a vortex convecting in a uniform compressible flow with velocity U under a profile. The aerodynamic loads generated by this vortex under the profile are studied. In the model studied, the vortex is considered to be thrown 30 chords of distance ahead of the profile, with vortex intensity gone through a dimensionless process by uniform flow and chord of $\Gamma/Uc = 0.2$, and still, the vortex located down the $1/4c$ profile. These values were chosen to allow comparison with the study of Sitaraman and Baeder [27]. Figure 7 shows the AVI problem schematic.

Because the vortex is thrown at a relatively large distance (in terms of nonstationary effects) of the profile, $30c$, the simplifying hypothesis of incompressible vortex is considered; its effects at the initial instants can be considered small and, when near the profile, it would have already reached the steady flow. Figure 8 shows the vortex-induced velocity that moves in the flow velocity to a position 30 chords ahead of its origin, that is, the leading edge of the considered AVI schematic. Figure 8 shows that, at this distance, the compressible and incompressible vortex-induced velocities are the same, allowing us to adopt the hypothesis of incompressible vortex without mistakes. However, this fact constitutes a limitation of the model in relation to the launching position of the vortex, and this effect should be the aim of future studies. Still, because the model considers the convecting vortex a theoretical vortex (Biot–Savart [2]), it does not suffer deformation when near the profile; Lee and Smith [35] studied this deformation.

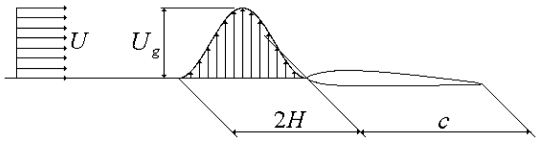

Fig. 5 One-minus-cosine gust.

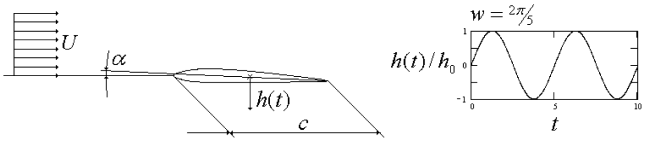

Fig. 6 Harmonic translation movement.

In an analogous way, a velocity ratio, λ, is defined for the sharp edge gust of the same formulation and physical sense. The boundary condition is given by the incompressible point vortex equation, in such a way that normal velocity induced over the profile is given by

$$w_v = -\frac{\Gamma}{2\pi}\frac{x_v - x}{(x_v - x)^2 + y_v^2}, \qquad \Gamma = 0.2Uc, \qquad x_v = 30c$$
$$y_v = 0.25c \tag{10}$$

IV. Results and Discussion

The aerodynamic coefficients are presented and calculated numerically for both flows, sub- and supersonic. Numerical results are compared with the solutions available in the literature. For gust studies, the results are compared with Leishman [26] and Lomax [36] for subsonic flow and with Lomax et al. [21] for supersonic flow, the latter limited to $\lambda = 0$ and 1 due to the lack of results contained in the literature.

The aerodynamic coefficients of a profile subjected to one-minus-cosine and minus-sine gusts calculated in the present study are compared with the results of Zaide and Raveh [34] in the subsonic regime; no reference for comparison was found for the supersonic regime. The comparison of the results obtained by the lateral harmonic movement is a suggestion for a future study; a good reference is Timman et al. [37].

For the AVI study, our results are compared with the results of Sitaraman and Baeder [27] in subsonic flow; no reference of the AVI (or BVI) studies in supersonic flow was found.

Figure 9 shows the results obtained for a sharp edge gust with a variable gust propagation velocity in sub- and supersonic flows compared with other references. In the subsonic flow, the steady-state values are obtained only asymptotically. The same is not true for the supersonic flow. In fact, steady-state values are attained earlier as the supersonic Mach number increases. The overall behavior exists due to wave traveling, which is only in the downstream direction in supersonic flow and in both directions in the subsonic flow. A strict correspondence between both sub- and supersonic flows was observed for the values obtained and the references.

Figure 10 shows, for the initial instants of the motion, the results obtained in sub- and supersonic flows of the profile submitted to a sharp edge gust with a variable gust propagation velocity. Curves of the lift coefficient and the variation of the aerodynamic center of the profile are presented. Two curves from the lift coefficient graphics are noticed: $\lambda = 0.01$ (using 0.01 for numerical limitation, intending to show the behavior for $\lambda = 0$) and $\lambda = 1$, representing a sudden change in the angle of attack and sharp edge gust motions, the indicial solutions found in the literature. It is verified that, as the coefficient λ varies from 0 to 2, a series of intermediate curves between the curves for these coefficients are obtained. In subsonic flow, the lift coefficient peak value is associated to the noncirculatory portion (or impulsive) that tends to become extinguished, predominating the circulatory portion in the following instants, when the continuous lift

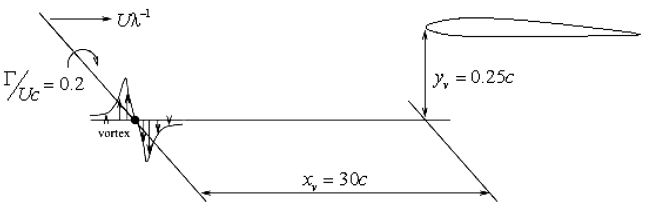

Fig. 7 AVI schematics.

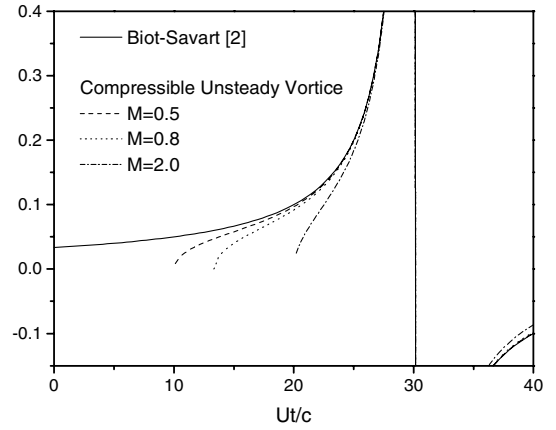

Fig. 8 Velocity induced by a vortex convecting with a uniform freestream flow velocity at a point situated at 30 chords ahead of its origin.

growth is verified. From the lift curves, it can be observed that, as the gust propagation velocity rises (an increase in λ), the noncirculatory portion peak is reduced and, at the same time, it lasts longer; this behavior is clear for $\lambda = 2$. The curves for supersonic flow show similar behavior, for which an increase in λ translates to a slower circulation growth. Figure 10d shows the time variation of the profile pressure center along the chord. In the subsonic case, the final position of the pressure center is in the quarter of the chord from the leading edge. In supersonic flow, the final position is at the halfway point of the profile chord. It can be noticed that a rise in λ implies a longer time for the steady flow to be reached. Again, this behavior is

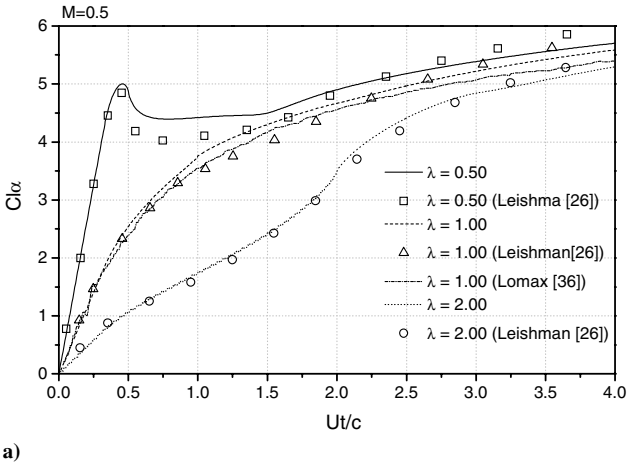

a)

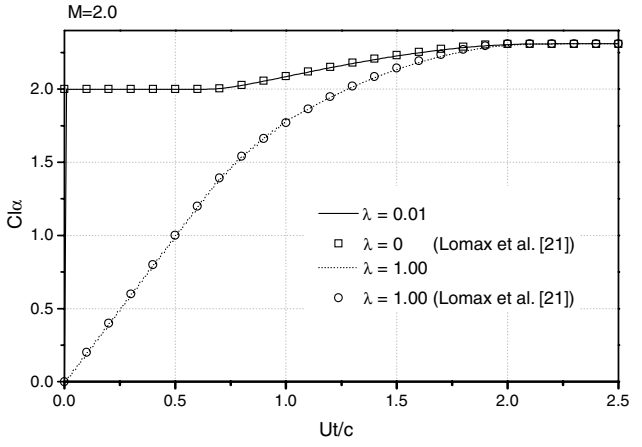

b)

Fig. 9 Sharp edge gust comparison: a) with Leishman [26] and Lomax [36] for subsonic flow, and b) with Lomax et al. [21] for supersonic flow.

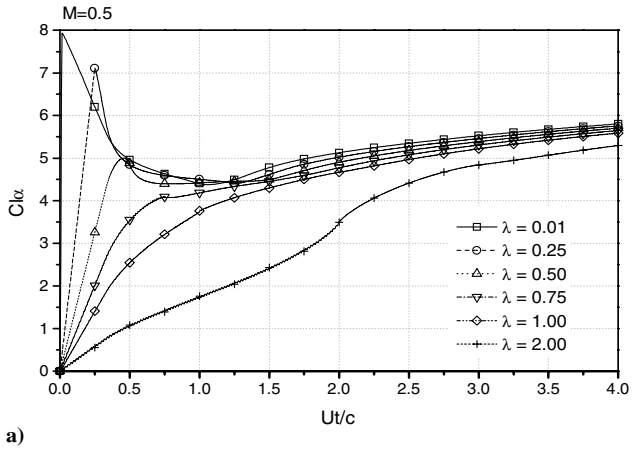

a)

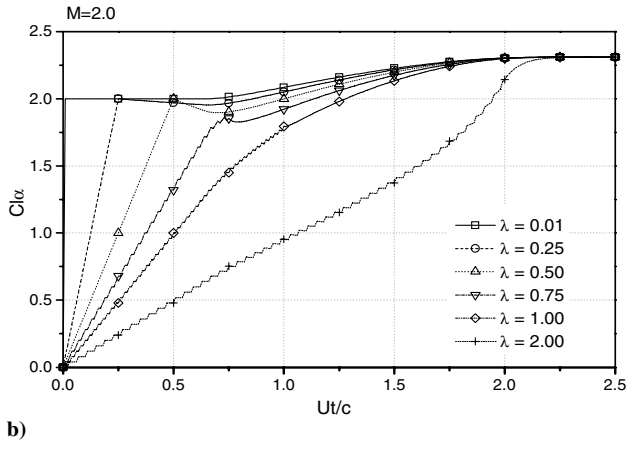

b)

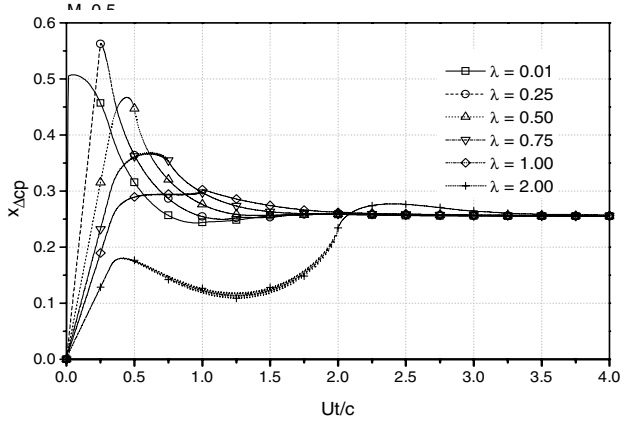

c)

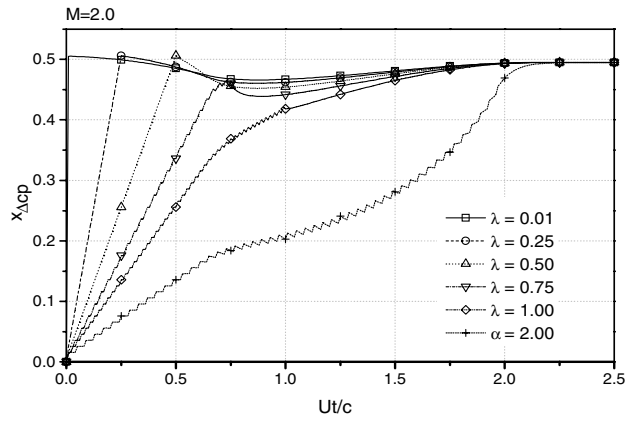

d)

Fig. 10 Sharp edge gust for several λ: a) lift for subsonic flow, b) lift for supersonic flow, c) pressure center for subsonic flow, and d) pressure center for supersonic flow.

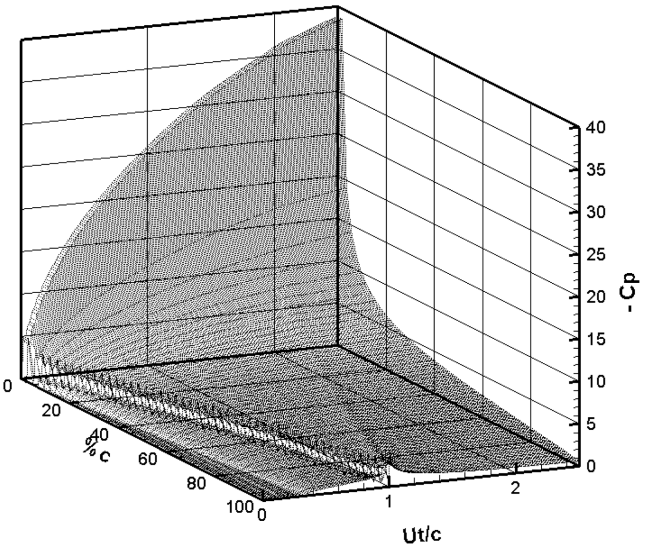

a)

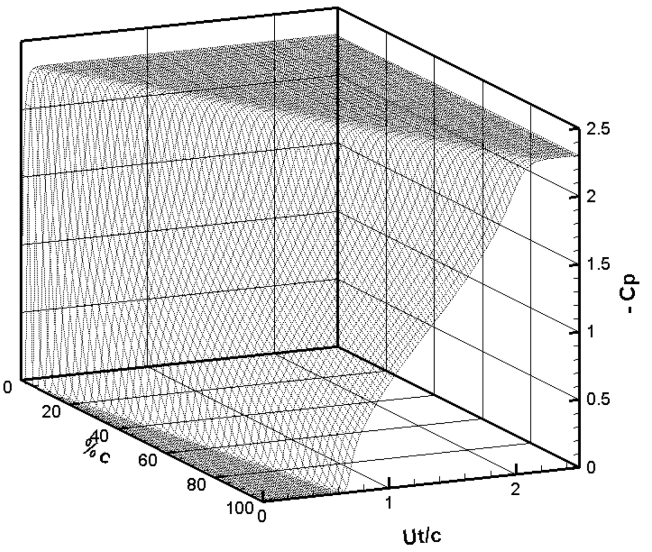

b)

Fig. 11 Distribution of the pressure coefficient jump over the profile for a sharp edge gust: a) subsonic flow ($M = 0.5$), and b) supersonic flow ($M = 2.0$).

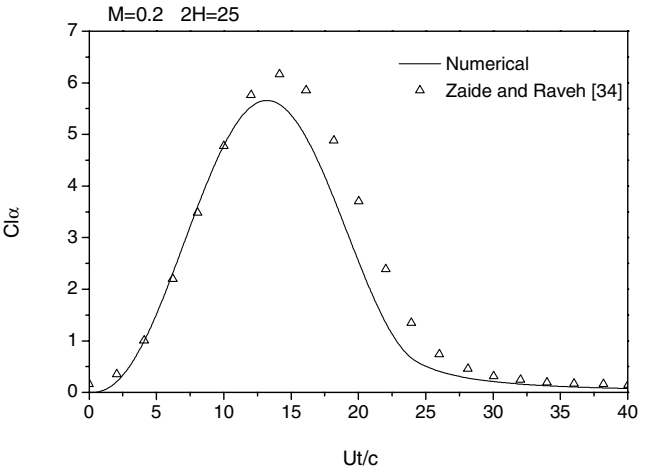

Fig. 12 Comparison of the one-minus-cosine gust with Zaide and Raveh [34].

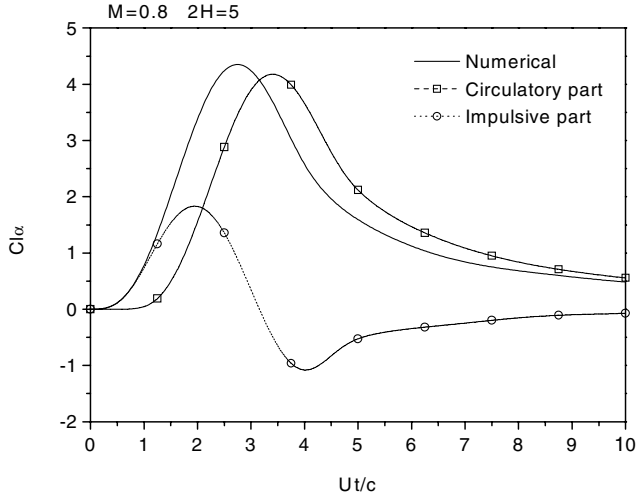

Fig. 13 One-minus-cosine gust for subsonic flow for $M = 0.8$.

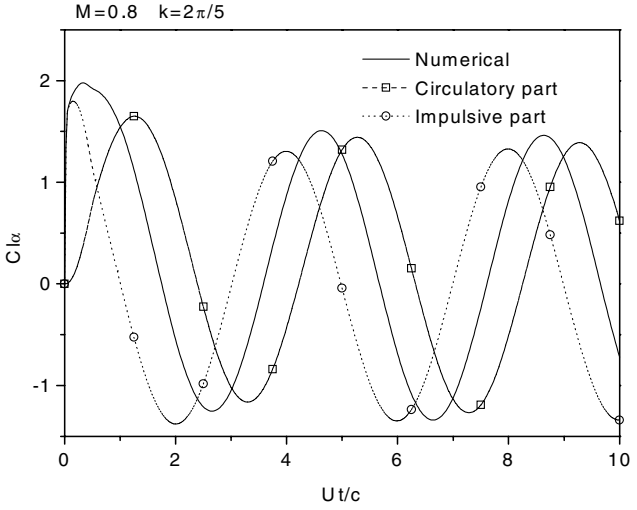

Fig. 15 Harmonic movement for the subsonic regime for $M = 0.8$.

explained by the fact that a rise in λ makes the circulatory portion grow in a slower way, taking, therefore, longer until a steady state is reached. A small oscillation in the curves is also verified in a higher magnitude for higher λ. This oscillation is numerically originated and occurs due to an oscillation in the pressure coefficient jump distribution curve over the profile (Hernandes and Soviero [33]), but it is not meaningful enough to invalidate the results. The variation of the pressure center must be taken into account in simplified versions of the vortex lattice method, for which a unit discretization is used along the chord, as in the Weissinger method.

Figure 11 shows an evolution of the pressure coefficient jump in time over the profile. A line that begins at the origin and ends in position $Ut/c = \lambda$ is clearly seen; this is the point at which the gust has run the profile as a whole. Following this condition, in subsonic flow, a predominant nonsteady region followed by a well-defined standard region is noticed, in which practically only the growing circulatory portion is observed. In the supersonic case, after the gust hit the whole profile, there is a region of high gradients that subsequently achieved steady flow; this is visible in the figures.

Figure 12 presents the gust results compared with the ones of Zaide and Raveh [34], which corroborates our results. For those specific gusts, a gust gradient of $2H = 25$ was considered.

Figure 13 shows the results obtained for the sustentation coefficient of the one-minus-cosine gust in the subsonic regime considering a gust gradient of $2H = 5$. The results are separated into two parts, circulatory and impulsive, also called steady and unsteady, respectively. The steady part is associated with the total circulation present over the profile at the considered moment, and the unsteady part is associated with the noncirculatory part, that is, the part that appears immediately after the presence of a perturbation potential velocity over the profile. It is noticed that the impulsive part is responsible for the early occurrence of a sustentation over the profile, because the circulation takes some time to be developed; the difference offset between the total sustentation and circulation sustentation is observed (the latter being late in comparison with the total). A difference in phase between the circulatory and impulsive parts is also noticed. This fact is also observed in the harmonic motion, studied here and discussed later.

Comparative results of both gusts for various velocities are shown in Fig. 14. It can be verified in both regimes (sub- and supersonic) that the closer the flow velocity is to the sound speed, the slower the return to the original sustentation value.

Figure 15 shows the results obtained for the sustentation coefficient of a profile submitted to the harmonic translation movement considering a gradient gust of $2H = 5$. The phases offset between the circulatory and impulsive parts are clear. This characteristic was shown by Theodorsen [32], in which the circulatory part is a function of the first time derivative and the impulsive part (noncirculatory) is a function of the second time derivative. A peak of the impulsive part in the beginning of the movement is also noticed. This behavior is due to the fact that a profile starts in rest and instantaneously begins the oscillatory movement. This characteristic, of an initial sustentation jump, is observed in the step function (Hernandes and Soviero [11]).

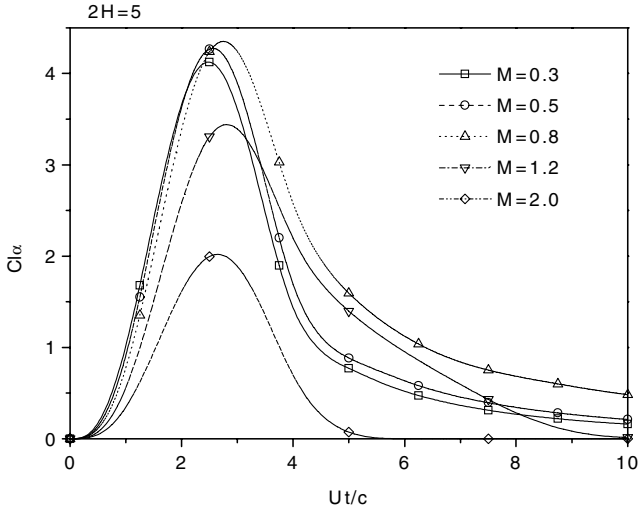

Fig. 14 Results for various gust velocities for the one-minus-cosine gust.

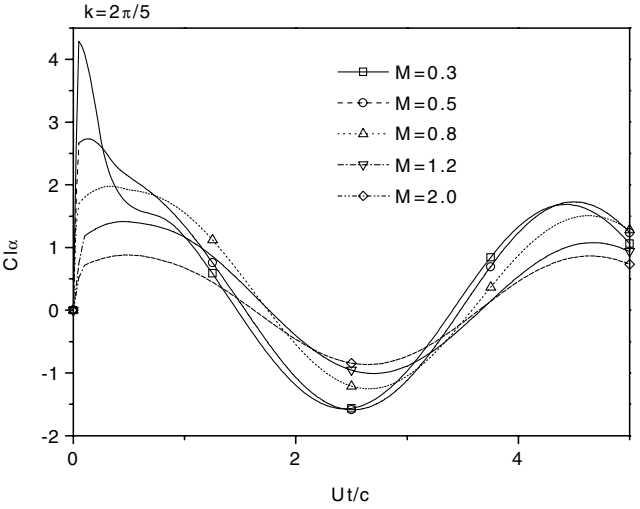

Fig. 16 Harmonic flow for various Mach numbers.

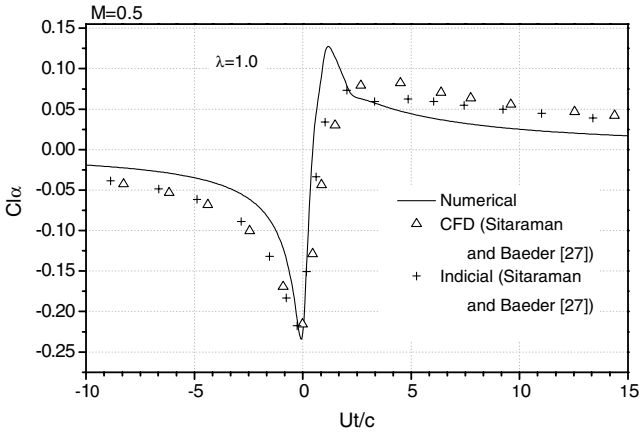

Fig. 17 Comparison of the AVI with Sitaraman and Baeder [27].

Figure 16 presents the results for the harmonic movement for various Mach numbers.

The results obtained for the AVI problem are shown in Figs. 17–20. Figure 17 shows the lift coefficients obtained compared with the values obtained by Sitaraman and Baeder [27], which corroborate our results. A small divergence in the positive peak value is observed, smaller for the values obtained via CFD and higher for the values obtained from approximated functions; these latter use exponential functions that normally cannot correctly translate the nonsteady peaks that exist in regions dominated by impulsive portion, those situated in regions next to the vortex position. It is possible to obtain a small improvement in the curve, approximating the CFD curve in the peak region, by raising the number of panels. Another point is that

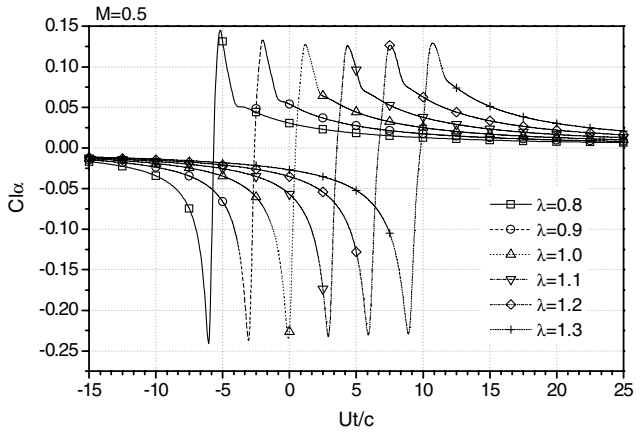

a)

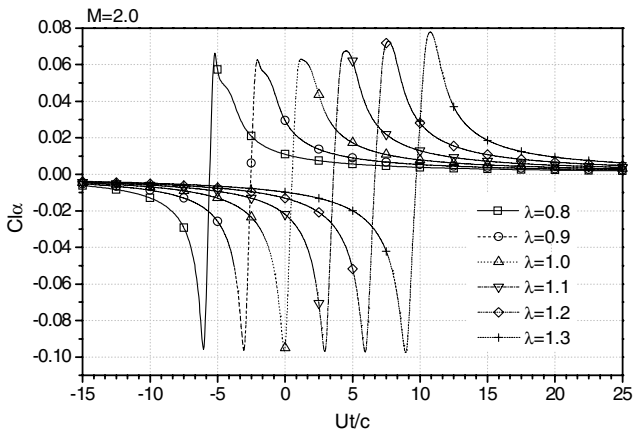

b)

Fig. 18 AVI for several λ: a) subsonic flow, and b) supersonic flow.

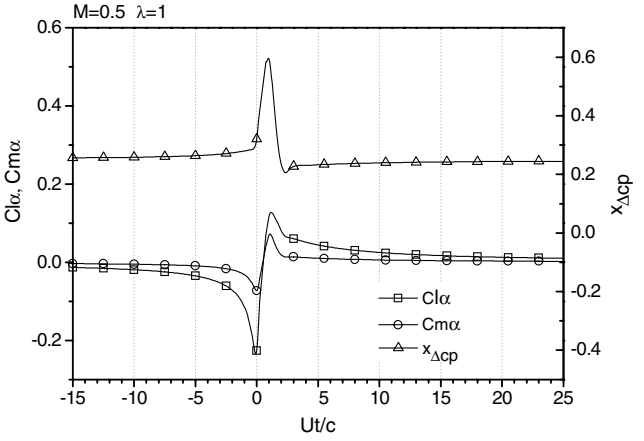

a)

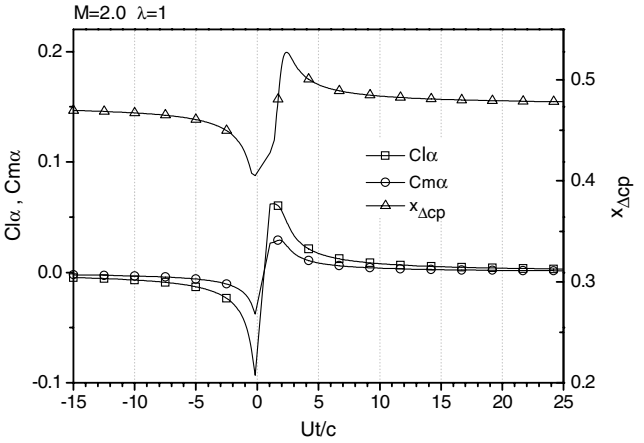

b)

Fig. 19 Lift, pitch moment, and evolution of the pressure center: a) subsonic flow, and b) supersonic flow.

Sitaraman and Baeder [27] used Scully's [38] vortex-core model to avoid a singularity at the center of the vortex. However, this small difference is only noticed in the peak region and it also has a high computational cost.

Figures 18 and 19 show the aerodynamic lift coefficients and the evolution of the pressure center for sub- and supersonic flows for several values of vortex propagation velocity. It is observed that the higher the values are of λ in subsonic flow, the lower the peaks are and the longer it will take for the lift to return to its initial value, a fact explained by the behavior that a rise in λ implies a higher smoothing of the impulsive portion and a slower growth of the circulatory portion. In supersonic flow, this behavior is not so evident. Still, as shown in Fig. 19, the time evolution of the profile pressure center

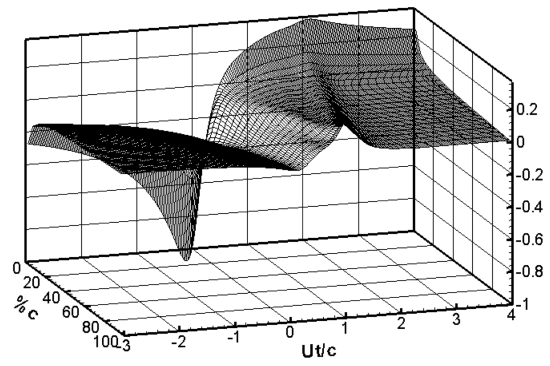

Fig. 20 Pressure jump coefficient distribution over the profile for the AVI problem for $M = 0.5$ and $\lambda = 1$.

obviously has its behavior directly affected by the vortex position over the profile.

Variations in the time of the pressure jump over the profile are shown in Fig. 20, with emphasis on the period during which the vortex passes over the profile in which the change on the lift signal occurs, highlighted by the inversion of the curves in the pressure distribution.

V. Conclusions

The aerodynamic coefficients are presented and numerically calculated for both sub- and supersonic flows. Numerical results are compared with the solutions available in the literature. For the gust study, the results are compared with Leishman [26] and Lomax et al. [21] for subsonic flow and to Bisplinghoff et al. [2] for supersonic flow, the latter limited to $\lambda = 0$ and $\lambda = 1$ due to the lack of results contained in the literature. The results of the aerodynamic coefficient of a profile subjected to one-minus-cosine and minus-sine gusts are compared with the results of Zaide and Raveh [34]. For the AVI study, the results are compared in subsonic flow with Sitaraman and Baeder [27].

The results show the compressibility effects of these problems, as well as how these motions are affected by the propagation velocity of the gust or vortex. The study of the airfoil–vortex interaction is the fundamental basis of studies on noise reduction of helicopters; this study is necessary for the development of more silent rotors.

The numerical method used here is, in fact, a natural extension of the compressible regime of the classical vortex lattice method in its two-dimensional version; it is the first methodology to use a simple numerical scheme to obtain forces and loads for an arbitrary motion of a profile in the unsteady compressible domain. The main physical difference is the finiteness of the disturbance propagations. The correspondence between vortex and normal dipole panels with constant density, as well as the concepts of bound and free vortices, remains valid in both sub- and supersonic regimes and is an essential feature of the numerical scheme.

Still, the present method obtained the results far faster (about 10,000 times faster) than if they had been obtained via CFD, and a significant correspondence between the obtained values and the references was observed; therefore, it is an excellent tool for a preliminary project on aircraft and helicopters.

Acknowledgments

The second author gratefully acknowledges the partial support of the National Council for Scientific and Technological Development, Brazil, under grant 302352/2002-3.

References

[1] Garrick, I. E., "Nonsteady Wing Characteristics," *High Speed Aerodynamics and Jet Propulsion*, Vol. 7, Sec. F, Princeton Univ. Press, Princeton, NJ, 1957, pp. 668–680.

[2] Bisplinghoff, R. L., Ashley, H., and Halfman, R. L., *Aeroelasticity*, Addison Wesley, Reading, MA, 1955, pp. 294–379.

[3] Bousquet, J., *Méthode des Singularités-Theorie et Applications*, Cepadues-Editions, Toulouse, France, 1990, pp. 92–107.

[4] Soviero, P. A. O., "Generalized Vortex Lattice Method for Oscillating Thin Airfoil in Subsonic Flow," *AIAA Journal*, Vol. 31, No. 12, 1993, pp. 2380–2382. doi:10.2514/3.11942

[5] Soviero, P. A. O., and Ribeiro, R. S., "Panel Method Formulation for Oscillating Airfoils in Supersonic Flow," *AIAA Journal*, Vol. 33, No. 9, 1995, pp. 1659–1666. doi:10.2514/3.12707

[6] Soviero, P. A. O., and Pinto, F. H. L., "Panel Method Formulation for Oscillating Airfoils in Sonic Flow," *Journal of the Brazilian Society of Mechanical Sciences*, Vol. 23, No. 4, 2001, pp. 401–409. doi:10.1590/S0100-73862001000400002

[7] Lomax, H., "Indicial Aerodynamics," *AGARD Manual on Aeroelasticity*, Pt. 2, AGARD, Neuilly-sur-Seine, France, 1960, Chap. 6.

[8] Heaslet, M. A., and Lomax, H., "Supersonic and Transonic Small Perturbation Theory," *High Speed Aerodynamics and Jet Propulsion*, Vol. 6, Sec. D, Princeton Univ. Press, Princeton, NJ, 1957, pp. 275–314.

[9] Long, N. L., and Watts, G. A., "Arbitrary Motion Aerodynamics Using an Aeroacoustic Approach," *AIAA Journal*, Vol. 25, No. 11, 1987, pp. 1442–1448. doi:10.2514/3.9802

[10] Morino, L., "A General Theory of Unsteady Compressible Potential Aerodynamics," NASA CR-2464, 1974.

[11] Soviero, P. A. O., and Hernandes, F., "Compressible Unsteady Vortex Lattice Method for Arbitrary Two-Dimensional Motion of Thin Profiles" *Journal of Aircraft*, Vol. 44, No. 5, 2007 pp. 1494–1498. doi:10.2514/1.27441

[12] Sears, W. R., *General Theory of High Speed Aerodynamics: High Speed Aerodynamics and Jet Propulsion*, Vol. 6, Princeton University Press, Princeton, NJ, 1954, p. 758.

[13] Mirels, H., and Haefeli, R. C., "The Calculation of Supersonic Downwash Using Line Vortex Theory," *Journal of the Aeronautical Sciences*, Jan. 1950, pp. 13–21.

[14] Hernandes, F., and Soviero, P. A. O., "Numerical Model for Thin Airfoils in Unsteady Supersonic Flow," *Proceedings of the 9th Brazilian Congress of Thermal Engineering and Sciences*, Brazilian Society of Mechanical Sciences and Engineering, Rio de Janero, 2002, p. 7.

[15] Miranda, L. R., Elliot, R. D., and Baker, W. M., "A Generalized Vortex Lattice Method for Subsonic and Supersonic Flow Applications," NASA Contractor Rept. 2865, 1977.

[16] Wagner, H., "Uber die Entstehung des Dynamischen Auftriesbes von Tragflugeln," *Zeitschrift für Angewandte Mathematik und Mechanik*, Vol. 5, No. 1, 1925, pp. 17–35. doi:10.1002/zamm.19250050103

[17] Küssner, H. G., "Zusammenfassender Bericht Under den Instationarem Auftreib von Flugeln," *Luftfahrtforschung*, Vol. 13, No. 20, 1936, pp. 410–424.

[18] Miles, J. W., "The Aerodynamic Force on an Airfoil in a Moving Gust," *Journal of the Aeronautical Sciences*, Vol. 23, 1956, pp. 1044–1050.

[19] Drischler, J. A., and Diederich, F. W., "Lift and Moment Responses to Penetration of Sharp-Edged Traveling Gusts, with Application to Penetration of Weak Blast Waves," NACA TN 3956, 1957.

[20] Soviero, P. A. O., and Lavagna, L. G. M., "A Numerical Model for Airfoils in Unsteady Motion," *Journal of the Brazilian Society of Mechanical Sciences*, Vol. 19, No. 3, 1997, pp. 332–340.

[21] Lomax, H., Heaslet, M. A., Fuller, F. B., and Sluder, L., "Two- and Three-Dimensional Unsteady Lift Problems in High-Speed Flight," NACA Rept. 1077, 1952.

[22] Heaslet, M. A., and Lomax, H., "Two-Dimensional Unsteady Lift Problems in Supersonic Flight," NACA Rept. 945, 1947.

[23] Shaw, T. S., and Qin, N., "Calculation of Compressible Indicial Response," *The Aeronautical Journal*, Dec. 2000, pp. 665–673.

[24] Beddoes, T. S., "Practical Computation of Unsteady Lift," *Vertica*, Vol. 8, 1984, pp. 55–71.

[25] Leishman, J. G., "Subsonic Unsteady Aerodynamics Caused by Gusts Using the Indicial Method," *Journal of Aircraft*, Vol. 33, No. 5, 1996, pp. 869–879. doi:10.2514/3.47029

[26] Leishman, J. G., "Unsteady Aerodynamics of Airfoils Encountering Traveling Gusts and Vortices," *Journal of Aircraft*, Vol. 34, No. 6, 1997, pp. 719–729. doi:10.2514/2.2250

[27] Sitaraman, J., and Baeder, J. D., "Computational-Fluid-Dynamics-Based Enhanced Indicial Aerodynamic Models," *Journal of Aircraft*, Vol. 41, No. 4, 2004, pp. 798–810. doi:10.2514/1.12419

[28] Noback, R., "Comparison of Discrete and Continuous Gust Methods for Airplane Design Loads Determination," *Journal of Aircraft*, Vol. 23, No. 3, 1986, pp. 226–231. doi:10.2514/3.45293

[29] Pratt, K. G., and Walker, W. G., "A Revised Gust-Load Formula and a Re-Evaluation of V-G Data Taken on Civil Transport Airplanes From 1933 to 1950," NACA Technical Rept. 1206, 1954.

[30] Flomenhoft, H. I., "Brief History of Gust Models for Aircraft Design," *Journal of Aircraft*, Vol. 31, No. 5, 1994, pp. 1225–1227. doi:10.2514/3.46637

[31] Fuller, J. R., "Evolution of Airplane Gust Loads Design Requirements," *Journal of Aircraft*, Vol. 32, No. 2, 1995, pp. 235–246. doi:10.2514/3.46709

[32] Theodorsen, T., "General Theory of Aerodynamic Instability and the Mechanism of Flutter," NACA Technical Rept. 496, 1935.

[33] Hernandes, F., and Soviero, P. A. O., "A Numerical Model for Thin Airfoils in Unsteady Compressible Motion," *Proceedings of the 10th Brazilian Congress of Thermal Engineering and Sciences*, Brazilian

Society of Mechanical Sciences and Engineering, Rio de Janero, 2004, p. 12.

[34] Zaide, A., and Raveh, D., "Numerical Simulation and Reduced-Order Modeling of Airfoil Gust Response," AIAA Paper 2005-5128, 2005.

[35] Lee, D. J., and Smith, C. A., "Effect of Vortex Core Distortion on Blade-Vortex Interaction," *AIAA Journal*, Vol. 29, No. 9, 1991, pp. 1355–1362.
doi:10.2514/3.10746

[36] Lomax, "Lift Developed on Unrestrained Rectangular Wings Entering Gusts at Subsonic and Supersonic Speeds," NACA Rept. 1162, 1954.

[37] Timman, R., van de Vooren, A. I., and Greidanus, J. H., "Aerodynamic Coefficients on an Oscillating Airfoil in Two-Dimensional Subsonic Flow," *Journal of the Aeronautical Sciences*, Vol. 18, No. 12, 1951.

[38] Scully, M. P., "Computation of Helicopter Rotor Wake Geometry and Its Influence on Rotor Harmonic Airloads," Department of Aerospace Engineering, Massachusetts Inst. of Technology ASRL TR 178-1, Cambridge, MA, March 1975.